Carbonates and Evaporites (2025) 40:48
https://doi.org/10.1007/s13146-025-01087-z

ORIGINAL ARTICLE

Mechanisms for overpressure generated by the undercompaction involving halite in Shale-sand layers

Taozheng Yang[1,2] · Chenglin Liu[1,2] · Jixian Tian[3] · Rizwan Sarwar Awan[4] · Guoxiong Li[5] · Zhengang Ding[1,2] · Hongliang Huo[1,2] · Yubo He[1,2] · Haidong Wang[1,2] · Tong Qiao[1,2]

Accepted: 21 March 2025

Abstract
High Shale content, a high sedimentation rate, and a sequence of initially slow followed by rapid sediment deposition are widely considered favorable conditions for the formation of overpressure. These conditions are also applicable in layers containing halite. The role of halite in the formation and evolution of overpressure remains unclear. This study relies on mathematical and numerical simulations to investigate the overpressure phenomenon in simplified geometric structures of shale-sandstone layers with halite. Our findings confirm that the basic mechanism involves the influence of halite on rock properties within the shale-sandstone layers. The occurrence of halite in rock layers alters the compaction curve of the rocks, causing a reduction in rock permeability. These findings not only advance the timing of overpressure occurrence in the layer but also intensify its magnitude. Due to the presence of halite, the threshold of mudstone content that forms overpressure in the layer decreases compared with non-saline layers. As a result, overpressure phenomena may occur in layers that previously did not meet the conditions for overpressure formation. We also found that the higher the halite content, the less influence of sedimentation rate and sedimentation mode on overpressure formation. In addition, this study also clarifies the role of gypsum in the formation of overpressure, and believes that the thickness of gypsum is the key factor in determining the magnitude of overpressure.

Keywords Undercompaction · Halite · Sedimentation rate · Deposition method · Numerical simulation

Introduction

Overpressure is a common phenomenon in oil and gas-bearing basins. Globally, more than 180 such basins have been discovered, with over 90% containing oil and gas (Du et al. 1995; Hunt 1990). The development of overpressure results from an imbalance in formation pressure caused by blocked fluid flow in rock pores (Cao et al. 2006; Osborne and Swarbrick 1997; Ramdhan and Goulty 2018), which significantly impacts the generation, migration, accumulation and preservation of oil and gas in the sedimentary basin (Liu et al. 2017; Shi et al. 2015). Due to the rapid deposition of the formation, the permeability of the sediment quickly decreases, hindering the flow of pore fluids. Consequently, the rate of increase in effective stress within the formation diminishes, causing the pore fluid to bear part of the pressure from the overlying formation. This leads to the formation of undercompaction overpressure (Dickinson 1953; Feng and Cai 2014; Wang et al. 2012). Although the idea that disequilibrium compaction causes overpressure has

✉ Chenglin Liu
liucl@cup.edu.cn

1 State Key Laboratory of Petroleum Resources and Prospecting, China University of Petroleum, Beijing 102249, China

2 College of Geosciences, China University of Petroleum, Beijing 102249, China

3 Research Institute of Petroleum Exploration and Development, Beijing 100083, China

4 School of Resources and Environmental Engineering, Hefei University of Technology, Hefei, Anhui Province 230009, China

5 Oil and Gas Technology Research Institute, PetroChina Changqing Oilfield Company, Xi'an 710018, China

Published online: 02 April 2025

recently been questioned (Li et al. 2020; Zhao et al. 2017), most scholars still believe that undercompaction is one of the primary mechanisms for generating large-scale overpressure (Broichhausen et al. 2005; Kukla et al. 2011; Liu et al. 2019c; Luo 2000), This phenomenon typically develops in thick, rapidly deposited shale formations with low permeability (Cao et al. 2006; Ramdhan and Goulty 2010). The leading causes of overpressure include massive sedimentary thickness, high depositional rates, and the absence of permeable layers (Yang et al. 2015). Generally, the presence of disequilibrium compaction can be identified by analyzing the rate of sediment deposition and correlating it with the presence of an abnormal acoustic curve. However, studying a single factor alone cannot provide reliable evidence of overpressure (Wang et al. 2011). For instance, the Malay Basin, a rift basin, developed rapidly during the Cenozoic era with a maximum deposition rate of 1000 m/Ma. Yet, its overpressure origin is primarily attributed to hydrocarbon generation supercharging (Tingay et al. 2013).

Many simulation software programs have been developed to better understand the complex geological phenomena occurring during the development and evolution of a basin and to model its physicochemical aspects (Luo and Vasseur 2016). Fluid pressure results from various generation mechanisms, such as mechanical compaction, tectonic stress, fluid expansion, and chemical reactions, that increase pressure in a given formation (Fan et al. 2016; Su et al. 2019). For the compaction mechanism produced by overpressure, the pressure state and evolution of the shale in the model (pressure increase, retention, and dissipation) depend on the hydraulic flow of tiny pores with the weight of the overburden on one side (Liu et al. 2016). Similarly, for the compaction mechanism induced by overpressure, the shale's pressure state and evolution in the model are influenced by the hydraulic flow in tiny pores and the overburden's weight (Audet and McConnell 1992; Neuzil and Pollock 1983).

The formation of halite and gypsum rocks is a characteristic feature of saline strata. Recently, scholars have recognized that saline lake basins exhibit unique petroleum geological conditions and accumulation characteristics distinct from those of freshwater lake basins (Guo et al. 2018). Previous studies on overpressure in salt lake basins have mostly focused on the positive role of gypsum in preserving overpressure, while for halite, the focus has been on its process, but the impact on overpressure has rarely been mentioned (Wang et al. 2022). For instance, pressure analysis of the Yingxi area in the Qaidam Basin indicates that an increase in the cumulative thickness of gypsum-salt rocks corresponds to a higher formation pressure coefficient, with values exceeding 2.0 in some cases (Li et al. 2021). Li and Zhao (2012) observed that significant overpressure in the Liutun Depression developed under a notably low sedimentation rate, which was much lower than that of the Yinggehai Basin, and they concluded that the primary factor driving the undercompaction of the strata was the highly effective sealing capability of the gypsum layer. Liu et al. (2020) discovered that the gypsum layer in the Dongpu Depression serves as a reliable marker for overpressure boundaries. A notable characteristic of salt lake sedimentary basins is their extremely high pressure coefficients, with values exceeding 1.6 in formations where gypsum and salt rocks co-occur, and reaching above 2.0 in some cases. This raises the question: is the occurrence of such abnormally high formation pressures in salt lake basins linked to the presence of salt? If so, what role does salt play in the mechanisms driving overpressure development?

Methods

In this paper, the numerical basin modeling software "PetroMod" is used as a quantitative analysis tool to simulate overpressure formation during compaction. The basin simulation method mainly uses the reverse stripping method to reconstruct the paleo-pressure. Then current thickness and pressure of a given formation are reconstructed into the thickness and pressure observed at a certain time during the deposition or burial process. The sedimentary profile shown in Fig. 1 consists of a 5350 m thick rock bed with an impervious foundation at its base.

The following are the basic assumptions for the development of the current basin model: (1) There is no uplift, denudation, chemical reactions, tectonic stress, or fluid expansion in the sedimentary profile to ensure that any pressure changes are solely due to compaction. (2) The rock is considered isotropic, and throughout the burial process, the rock particles and pore space have not reached their compression limits. (3) The rocks in the simulation are a mixture of shale, sandstone, and halite in specific proportions. The parameters for each rock type in the software are shown in Table 1 (DR = deposition rate; SHC = shale content; SAC = sandstone content; HAC = halite content; SHC + SAC + HAC = 100%). (4) Point A at a depth of 5000 m was selected on the two-dimensional sedimentary profile to illustrate the overpressure process in the entire compaction history (Fig. 1).

In this study, we simulated the formation of overpressure development processes for different lithological components, deposition rates, and deposition methods. By analyzing the current fluid pressure distribution characteristics of the vertical section (Fig. 1) and the residual pressure evolution history of point A, we identified the favorable factors for overpressure development. Additionally, we used the Yingxi area in the western Qaidam Basin as a case study

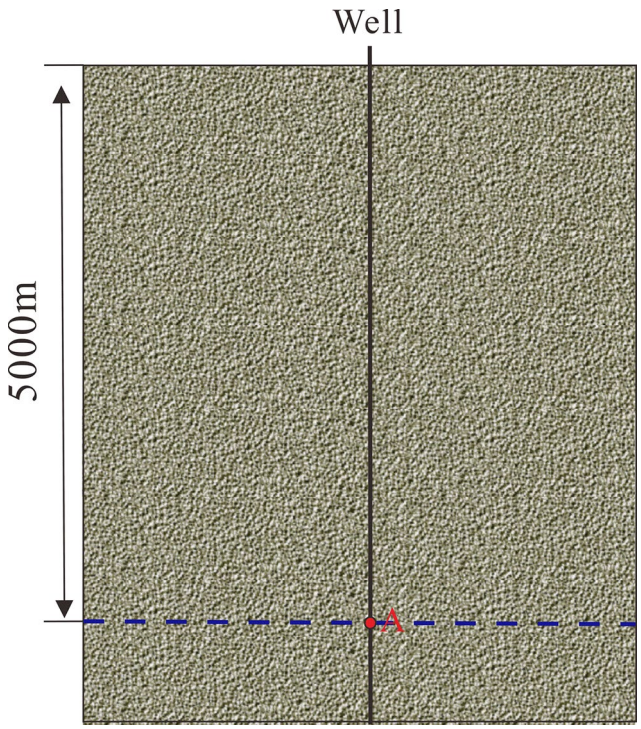

Fig. 1 Vertical section of the simulation model

Table 1 Constant terms for each component of the custom rock in this model

Rock property	Sandstone	Shale	Halite
ρ (g/cm^3)	2.72	2.7	2.2
g(m/s^2)	9.80	9.80	9.80
Eg (MPa)	60,000	60,000	60,000
$E_{\Phi m}$ (MPa)	60,000	60,000	60,000
$E_{\Phi i}$ (MPa)	25,000	15,000	20,000
Φm	45%	71%	-
Φi	4%	2%	-
c (m^{-1})	0.00031	0.00083	-
b (MPa^{-1})	0.0266	0.0961	-

to simulate the distribution characteristics of formation overpressure in wells S35 and S23. The final pressure in the simulation was constrained by measured pressure data. The results show a strong positive correlation between formation overpressure and the thickness of the gypsum rock.

The rocks in the software conform to the characteristics of an isotropic poroelastic model, where the difference between the static pressure of the rock mass and the effective stress determines the pore pressure. However, it should be noted that this formula, based on soil mechanics, is primarily applicable to unconsolidated materials. Therefore, when dealing with consolidated rock formations, it is necessary to incorporate a correction coefficient (Zhang 2013):

$$\sigma = P_h - \alpha P \tag{1}$$

Where: P and P_h represent the pore pressure and the lithostatic pressure (MPa), respectively. σ is the effective stress, and αis the Biot effective stress coefficient.

It is well known that overburden pressure is a function of depth:

$$P_h = \rho g Z \tag{2}$$

Where: ρ is the density of overlying strata (g/cm^3), g is the acceleration of gravity (m/s^2), and z is the depth (m).

The mechanical compaction model proposed by Athy was used to calculate the porosity (Athy 1930), and the compaction model can be expressed in the following two ways (Zhang 2011):

$$\Phi = \Phi i + (\Phi m - \Phi i)e^{-cz} \tag{3}$$

$$\Phi = \Phi i + (\Phi m - \Phi i)e^{-b\sigma} \tag{4}$$

The effective stress coefficient α of the customized rock is calculated by Bulk modulus of elasticity and grain modulus of elasticity (Luo et al. 2007):

$$\alpha = 1 - \frac{E\Phi}{Eg} \tag{5}$$

Where: E and Eg are the bulk modulus and grain modulus of elasticity (MPa), respectively. Based on the assumption of an isotropic rock medium, the bulk elastic modulus and Poisson's ratio of the rocks are calculated using the interpolation method:

$$V\Phi = \left[\frac{(V_{\Phi m} - V_{\Phi i})(\Phi - \Phi m)}{\Phi m - \Phi i)}\right] + V_{\Phi m} \tag{6}$$

$$E\Phi = \left[\frac{(E_{\Phi m} - E_{\Phi i})(\Phi - \Phi m)}{\Phi m - \Phi i)}\right] + E_{\Phi m} \tag{7}$$

Where: Φ is the porosity at a given depth, Φm is the original porosity, and Φi is the porosity at the ultimate compression state. V_Φ is the Poisson's ratio at a given depth, $V_{\Phi m}$ is the original Poisson's ratio, and $V_{\Phi i}$ is the Poisson's ratio at the ultimate compression state. Similarly, E_Φ is the bulk modulus of elasticity at a given depth, $E_{\Phi m}$ is the original bulk modulus of elasticity, and $E_{\Phi i}$ is the bulk modulus of elasticity at the ultimate compression state (MPa), c is the compaction coefficient (m^{-1}), b is the stress coefficient (MPa^{-1}).

Simultaneous formulae (1) ~ (7) can be employed to obtain the pore pressure (P) calculation formula as follows:

$$P = \frac{Eg - E\Phi}{Eg}\left(\frac{\rho g}{c} - \frac{1}{b}\right)\ln\left[\frac{\Phi m - \Phi i}{\Phi - \Phi i}\right] \tag{8}$$

Results and discuss

Compaction and porosity - permeability characteristics of "custom rocks"

The rock simulated in this study is a mixture of sandstone, shale, and halite in specific proportions. During the mixing process, different averaging methods are chosen based on the type of physical property (Hantschel et al. 2012; Wang et al. 2022). For instance, properties like porosity, Poisson's ratio, and density are treated as bulk parameters and are mixed using weighted arithmetic means, while permeability, being a transport parameter, is mixed using the geometric mean.

Figure 2 illustrates the changes in the depth-porosity curve and the porosity-permeability curve for sandstone and shale after the addition of halite. The pore-depth relationship of the lithological components follows Athy's compaction law (Athy 1930), and the porosity-permeability curve exhibits a typical two-stage characteristic. As the HAC increases, the original porosity of both shale and sandstone significantly decreases (as shown by the porosity at a depth of 0 m in Fig. 2A and C). The reduction in the original porosity of sandstone due to the presence of halite is notably greater than that of shale. Regarding the minimum porosity (the lowest porosity during compaction), the addition of halite reduces the minimum porosity of sandstone but has almost no effect on shale. A common observation for both sandstone and shale is that the depth at which the minimum porosity is reached increases with the HAC.

Analyzing the changes in the porosity-permeability curves after adding halite (Fig. 2B and D), it is evident that halite reduces the permeability of both sandstone and shale, with a more pronounced reduction as the proportion of halite increases. Additionally, the decline in sandstone permeability is more noticeable compared to shale. This can be attributed to the fact that pores in rocks can be categorized into "reservoir pores" and "connected pores." Halite blocks both types of pores, leading to reduced permeability. The blockage of reservoir pores is reflected in the decreased original porosity, while the blockage of connected pores is shown by the reduced permeability. Since sandstone particles are larger than shale particles, the pore-blocking effect during compaction is more pronounced in sandstone. Consequently, on the depth-porosity and porosity-permeability curves, halite has a greater impact on reducing the permeability and original porosity of sandstone compared to shale (Fig. 2).

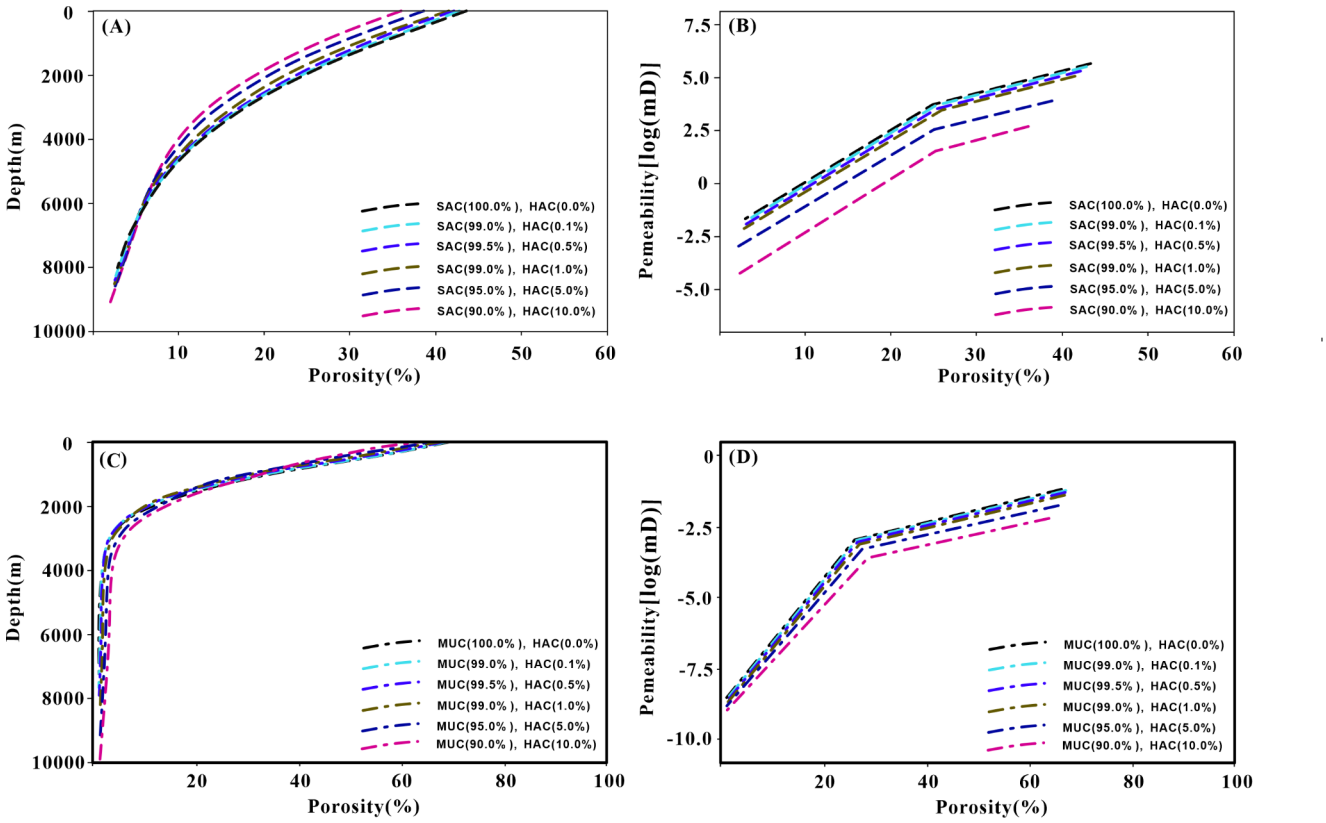

Fig. 2 Depth-porosity compaction curve and porosity-permeability curve

The influence of rock composition on overpressure

In clastic rock deposition, the rapid accumulation of low-permeability strata is crucial for the development of overpressure. The rate of deposition typically characterizes this rapid accumulation, while shale content plays a key role in controlling the permeability of the strata (Liu et al. 2019b). The above analysis indicates that the inclusion of halite influences the compaction and physical properties of the rock. However, the impact of adding halite on overpressure development remains uncertain. To investigate this, we used the vertical profile model (Fig. 1) and combined sandstone, shale, and halite in different proportions as outlined in Table 1. Each mixture resulted in a simulated current pressure distribution (Fig. 3) and the pressure evolution at point A (Fig. 4).

The Mudstone thickness/Layer thinkness (M/L) was set to five values: 0.5, 0.6, 0.7, 0.8, and 0.9. Additionally, for each of these five sand-shale ratios, we varied the salt content across six levels: 0.0%, 0.1%, 0.5%, 1.0%, 5.0%, and 10.0%. As illustrated in Figs. 3 and 4, we conducted a total of 30 simulations, with each simulation using a uniform deposition rate (DR) of 100 m/Ma. The specific content values for sandstone, shale, and halite used in the simulations are detailed in Appendix 1.

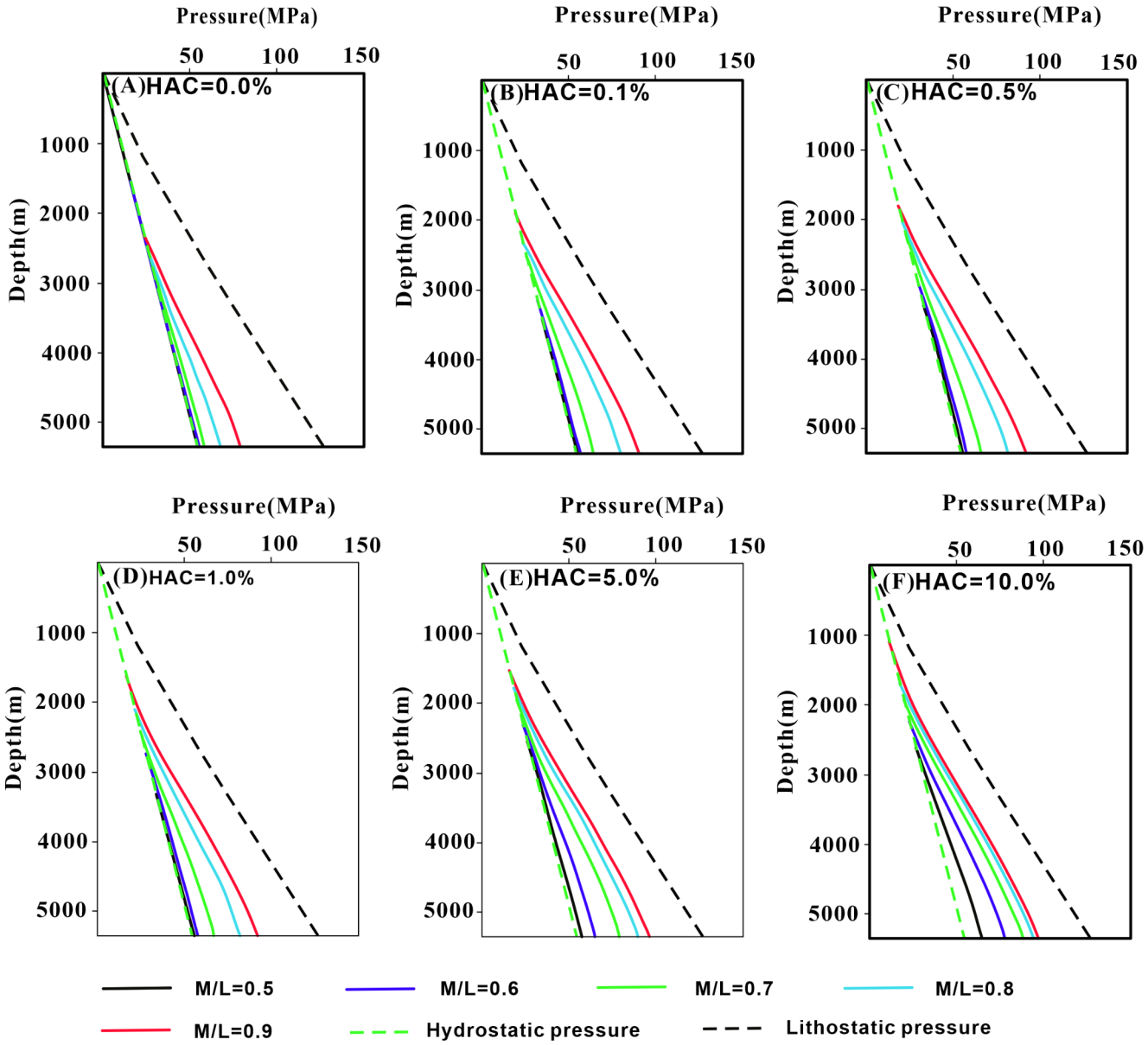

Fig. 3 Fluid pressure curve characteristics of different rock components: (**A**) HAC = 0.0%; (**B**) HAC = 0.1%; (**C**) HAC = 0.5%; (**D**) HAC = 1.0%; (**E**) HAC = 5.0%; (**F**) HAC = 10.0%

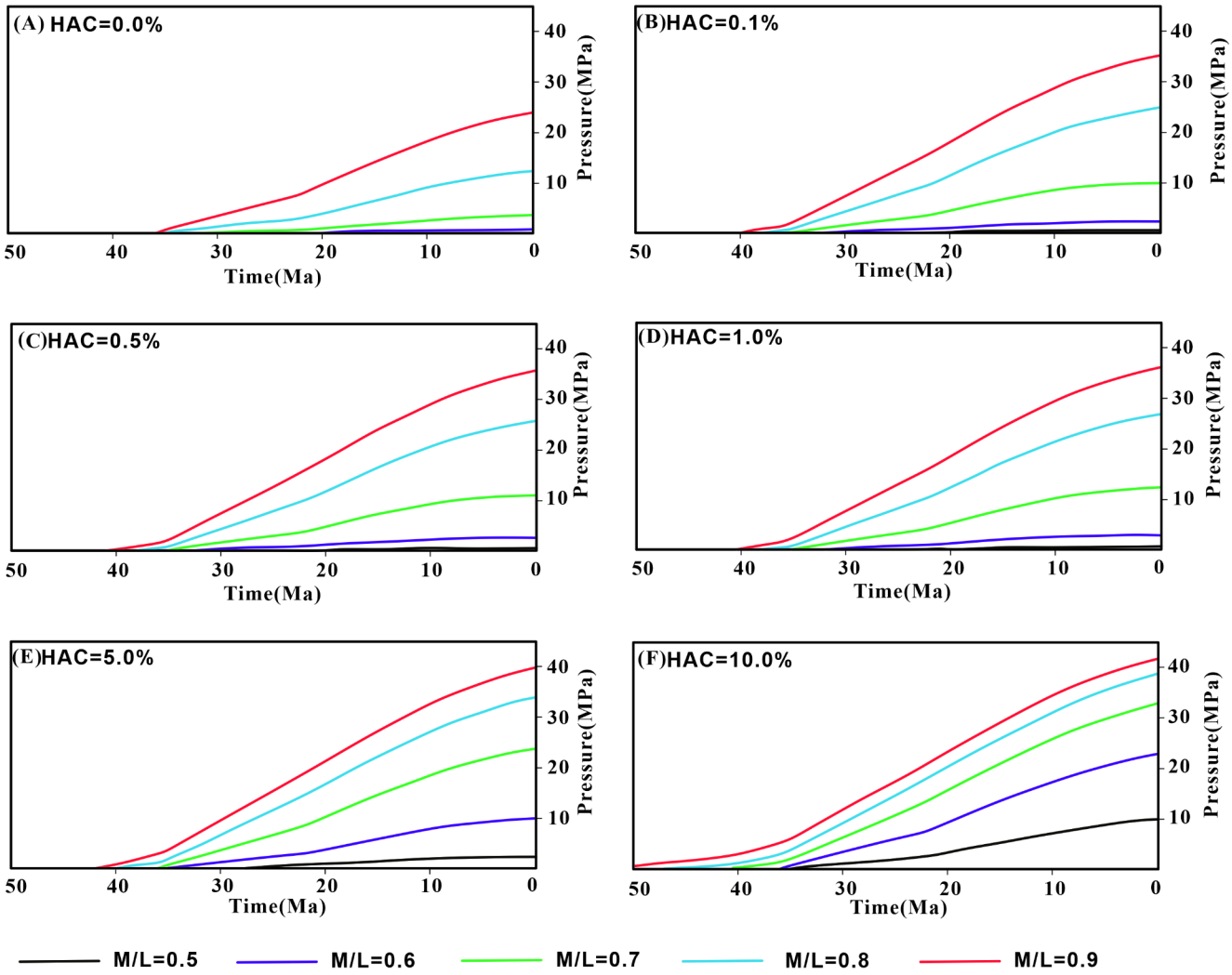

Fig. 4 Pressure evolution characteristics at point A: (**A**) HAC = 0.0%; (**B**) HAC = 0.1%; (**C**) HAC = 0.5%; (**D**) HAC = 1.0%; (**E**) HAC = 5.0%; (**F**) HAC = 10.0%

As shown in Fig. 3, a lower M/L corresponds to a higher intensity of overpressure. Additionally, the presence of halite significantly amplifies the overpressure intensity. Based on the results from the 30 simulations, when HAC = 0.0% (Fig. 3A), overpressure only forms when M/L is less than 0.7. Increasing the salt content raises the M/L threshold for overpressure formation. For instance, when the salt content is 1.0% (Fig. 3D), the M/L required for overpressure formation increases to 0.6. Further, when the salt content reaches 5.0% (Fig. 3F), the M/L threshold rises to 0.5.

As shown in Fig. 4, a lower M/L ratio leads to earlier onset and greater intensity of overpressure at point A. Increasing the HAC accelerates the timing of overpressure formation and amplifies its intensity. For example, with M/L = 0.7, when HAC = 0.0%, overpressure at point A begins forming at 30 Ma, reaching an intensity of 3.6 MPa. When HAC increases to 1.0%, overpressure begins at 35 Ma, with an intensity of 12.0 MPa. At 10.0% HAC, overpressure formation starts at 40 Ma, and the intensity rises to 33.1 MPa.

The effect of adding halite varies in terms of overpressure enhancement. For instance, when M/L = 0.9 and HAC = 0.0%, overpressure at point A starts at 36 Ma, with an excess pressure of 23.5 MPa (Fig. 4A). However, with HAC = 0.1%, overpressure begins at 40 Ma, increasing the excess pressure to 35.4 MPa (Fig. 4B). Conversely, with M/L = 0.6, even at 1% HAC, the overpressure formed at point A is negligible (Fig. 4D). But when HAC rises to 10%, overpressure appears at 35 Ma, reaching an intensity of 23.6 MPa (Fig. 4F).

The above analysis indicates that the formation of overpressure after adding custom halite follows these rules: (1) The higher the proportion of halite added, the higher the M/L at which overpressure begins to form, the earlier the overpressure onset, and the greater the intensity of overpressure. In other words, halite positively influences

overpressure development. (2) The impact of halite on overpressure enhancement varies. If the M/L is already near the lower limit for overpressure development, adding only a small amount of halite significantly enhances overpressure. However, if the rock does not meet the conditions for overpressure formation, a larger proportion of halite is required to induce overpressure.

The effect of deposition rate on overpressure

Previous studies believe that sedimentation rate is one of the key factors for overpressure (Fan and Wang 2021; Liu et al. 2019c). In actual basins, it is generally believed that overpressure of a certain magnitude can be developed at the depositional rate of 100 m/Ma in the low permeable layer (Liu et al. 2016). However, once the DR reaches the minimum threshold for overpressure formation, how does a further increase in DR affect overpressure? Does DR still play a decisive role in overpressure? In order to show the influence of DR on the development of overpressure, we take the case of M/L=0.8 as an example, and set the sedimentation rate to 100 m/Ma, 200 m/Ma, 300 m/Ma, 400 m/Ma and 500 m/Ma, a total of 5 different uniform sedimentation rates. At the same time, in order to reflect the influence of HAC on overpressure, we set 6 salt content gradients of HAC = 0.0%, HAC = 0.1%, HAC = 0.5%, HAC = 1.0%, HAC = 5.0% and HAC = 10.0%. Therefore. A total of 30 simulations were conducted, and the settings of each simulation are shown in Appendix 2.

The simulation results show that the current formation pressure gradually shifts to the right as the deposition rate increases (Fig. 5). In other words, the higher the DR, the greater the overpressure intensity. At the same time, we observed another phenomenon: the higher the HAC, the denser the formation pressure curve (Fig. 5).

As the salt content increases, the difference in the final pressure of point A in different curves becomes smaller and smaller (Fig. 6). For example, when HAC = 0.0%, the final pressure at point A is 11.5 MPa when the DR = 100 m/Ma, and the final pressure at point A increases to 20.7 MPa when the DR = 500 m/Ma, and the overpressure difference is 9.2 MPa. When HAC reaches 10.0%, the final pressure at point A is 35.8 MPa when the DR = 100 m/Ma, and the final pressure at point A increases to 37.8 MPa when the DR = 500 m/Ma, and the overpressure difference is reduced to 2.0 MPa. In other words, the halite component in the rock can dilute the effect of the sedimentation rate on the overpressure growth, and the higher the proportion of the halite component, the more obvious the dilution effect. For the overpressure formed during mechanical compaction, the greater the formation overpressure, the higher the degree of undercompaction of the formation. Obviously, the addition of halite enhances the rock's resistance to compaction, making the formation more prone to undercompaction. Our explanation is that halite fills the connected pores in the rock, resulting in a significant reduction in the rock's permeability. The HAC represents the filling efficiency of the connected pores in the rock. Therefore, the higher the HAC, the stronger the rock's ability to resist compaction.

The influence of deposition methods on overpressure

All the cases discussed above involve uniform formation deposition. However, in the actual depositional process, the formation's speed varies, and the influence of depositional mode on the formation and distribution of overpressure is unclear (Liu et al. 2019a). In order to reflect the influence of deposition mode on overpressure development, taking the case of M/L=0.8 as an example, three deposition modes are set: normal uniform deposition, fast first then slow deposition, and slow first then fast deposition. The burial process of thin layer A under different deposition modes is shown in Fig. 7. It should be noted that although there are differences in deposition modes, the average deposition rate is still 100 m/Ma. At the same time, in order to reflect the influence of HAC on overpressure, six salt content gradients are set: HAC = 0.0%, HAC = 0.1%, HAC = 0.5%, HAC = 1.0%, HAC = 5.0% and HAC = 10.0%. Therefore, a total of 18 simulations were carried out, and the rock composition settings for each simulation are shown in Appendix 3.

The simulation results for the rocks under three sedimentary modes reveal the following findings: the highest intensity of overpressure is observed in the first slow followed by fast depositional mode, followed by the uniform deposition, and the least intensity is observed in the first fast followed by slow deposition (Fig. 8). Large scale overpressure can be formed in the early stage of rapid deposition in the sedimentary mode of first fast followed by slow deposition, while the overpressure intensity increases gradually during the slow deposition stage. However, in the early slow depositional stage, overpressure usually does not form, but it increases rapidly during the fast depositional stage (Fig. 9). For strata that are first slowly deposited and then quickly deposited, although the slow deposition in the early stage of the strata is difficult to cause a rapid increase in formation pressure, after experiencing rapid burial in the later stage, there will be a stage of rapid growth in formation pressure. For the formations that are first deposited fast and then slow, although the early rapid deposition helps to form overpressure in the formation, the undercompaction strength formed is not large due to the shallow burial depth; and the slow deposition in the later stage leads to a significant slowdown in the increase process. Ultimately, the overpressure strength

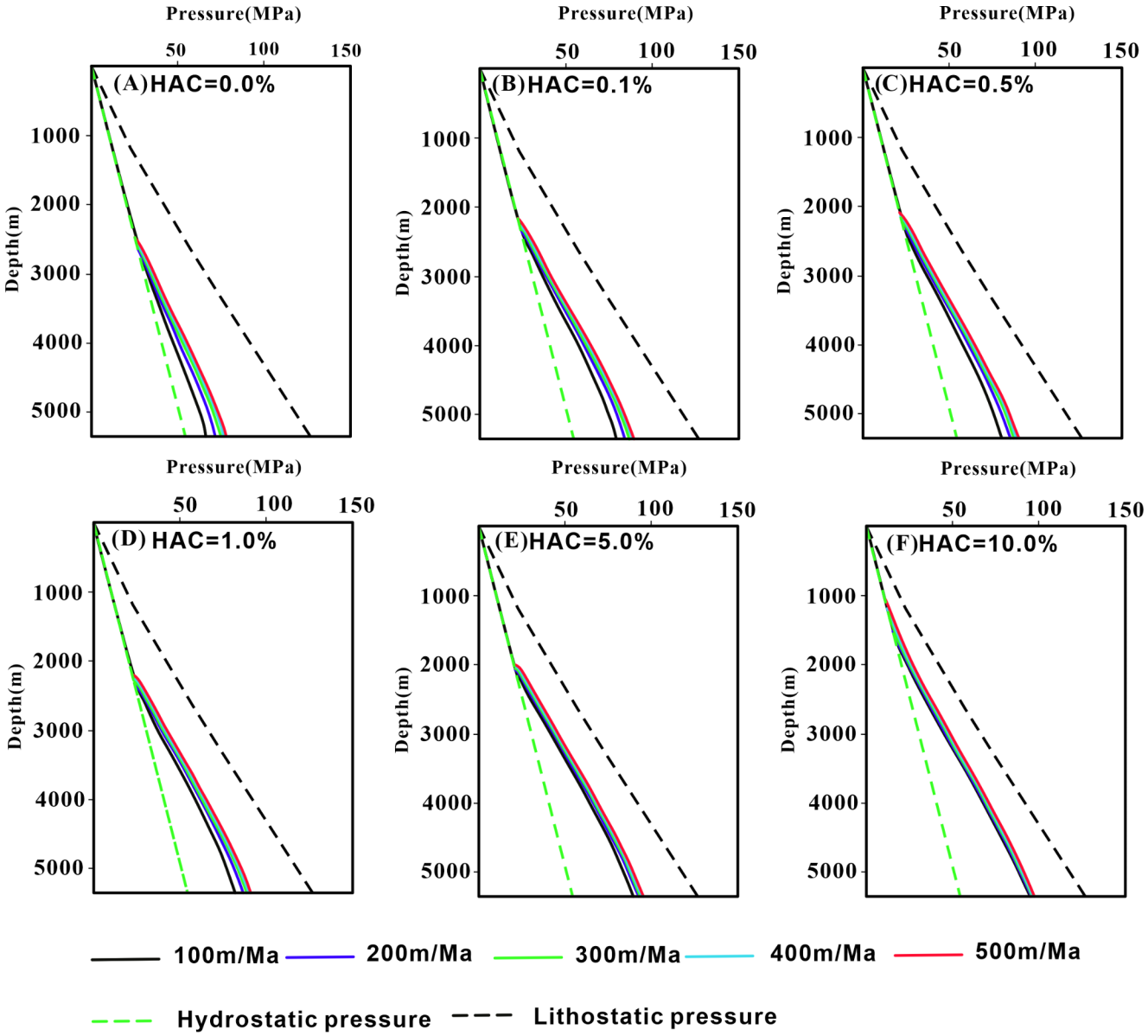

Fig. 5 Characteristics of fluid pressure curves at different sedimentation rates when SAC/SHC = 1/4: (**A**) HAC = 0.0% (**B**) HAC = 0.1%; (**C**) HAC = 0.5%; (**D**) HAC = 1.0%; (**E**) HAC = 5.0%; (**F**) HAC = 10.0%

is the highest in the slow-first-fast-later deposition mode, while the overpressure strength is the lowest in the fast-first-slow-later deposition mode. In fact, these early overpressures tend to have lower intensity, while higher intensity overpressures are characteristic of late stages, which aligns with geological facts (Zhao et al. 2017). This phenomenon occurs because, during the sedimentary process of geological bodies, the overpressure formed in the early stage is often destroyed by subsequent tectonic activities, resulting in pressure loss (Luo and Vasseur 2016; Luo 2004).

As the salt content increases, the fluid pressure curves under different deposition conditions continue to converge (Fig. 8). This feature is more obvious on the pressure evolution curve. For example, when HAC = 0.0% in the rock, the residual pressure difference caused by the deposition method is 6.6 MPa (see Fig. 9A). When HAC = 0.5% in the rock, the residual pressure difference caused by the deposition method is reduced to 5.1 MPa (see Fig. 9C). When the salt content in the rock increases to HAC = 5.0%, the residual pressure difference caused by the deposition method is further reduced to 2.3 MPa (see Fig. 9E). When the halite content in the rock further increases to HAC = 10.0%, the residual pressure difference caused by the deposition method is less than 0.9 MPa (see Fig. 9F). In other words, the addition of halite also dilutes the effect of the deposition method on overpressure, and the higher the

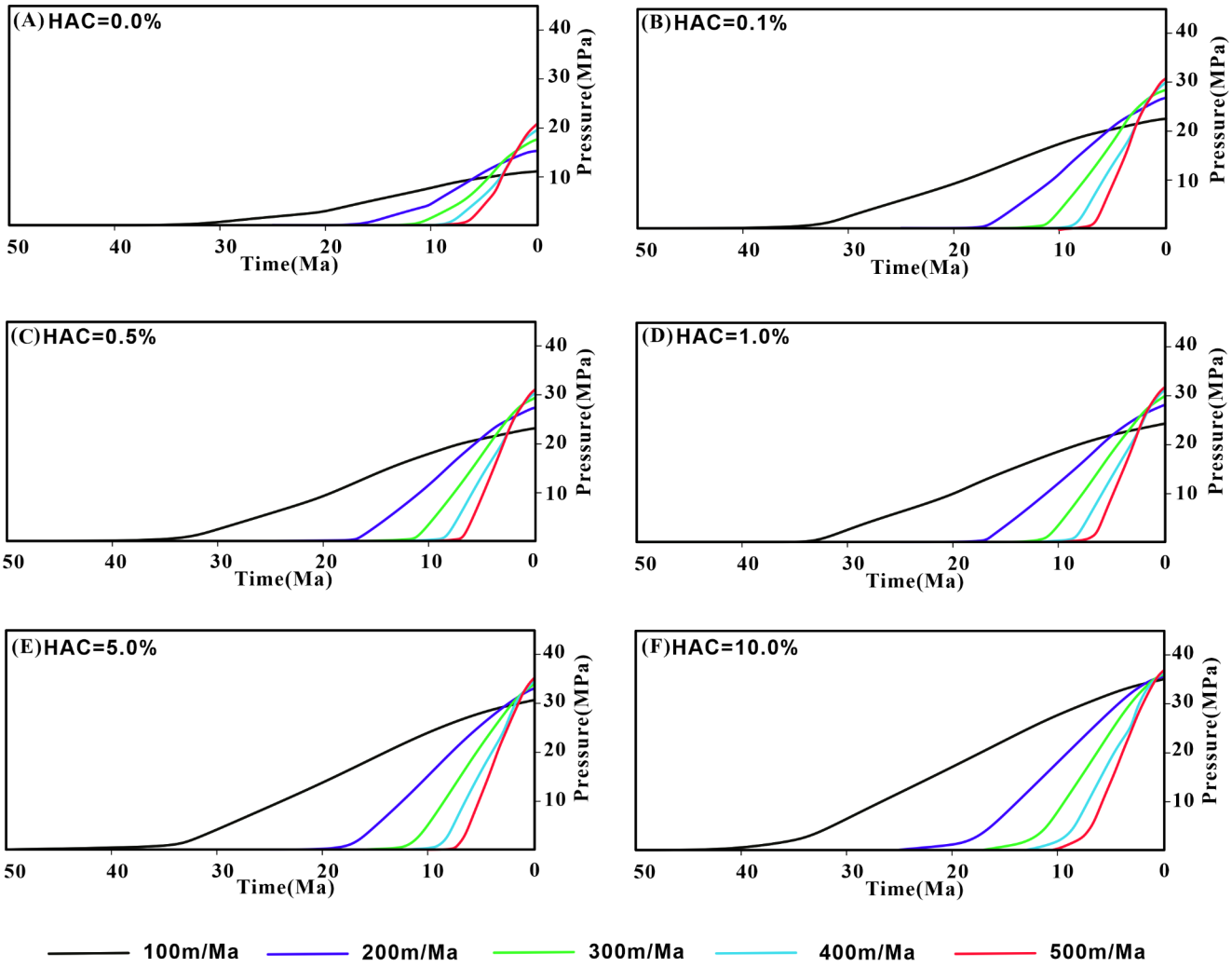

Fig. 6 Characteristics of fluid pressure evolution at point A at different deposition rates when SAC/SHC = 1/4: (**A**) HAC = 0.0%; (**B**) HAC = 0.1%; (**C**) HAC = 0.5%; (**D**) HAC = 1.0%; (**E**) HAC = 5.0%; (**F**) HAC = 10.0%

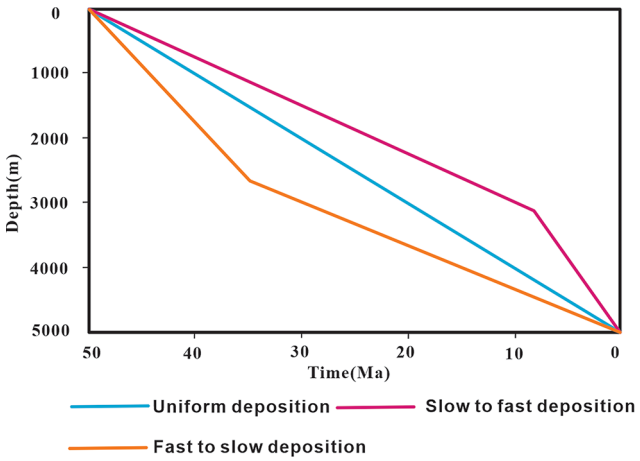

Fig. 7 Burial history of thin layer A under different sedimentary methods

salt content, the more obvious the effect. We believe that the effect of lithology on deposition method is consistent with the way it affects deposition rate. Halite enhances the compaction resistance of rock by filling the connected pores in the rock, and ultimately greatly reduces the effect of deposition rate on overpressure.

Case applications

This case study examines the overpressure results of the upper member of the Lower Ganchaigou Formation (E_3^2) in the western Qaidam Basin. It focuses on the relationship between the depositional rate, mineral composition, and present distribution characteristics of formation pressure in well Tu 2, Chaiye 2, Fengzhong 4 and Nan 14. The depositional rate is determined by dividing the ratio of formation thickness by the depositional time of the formation. The mineral composition, including halite content, clay

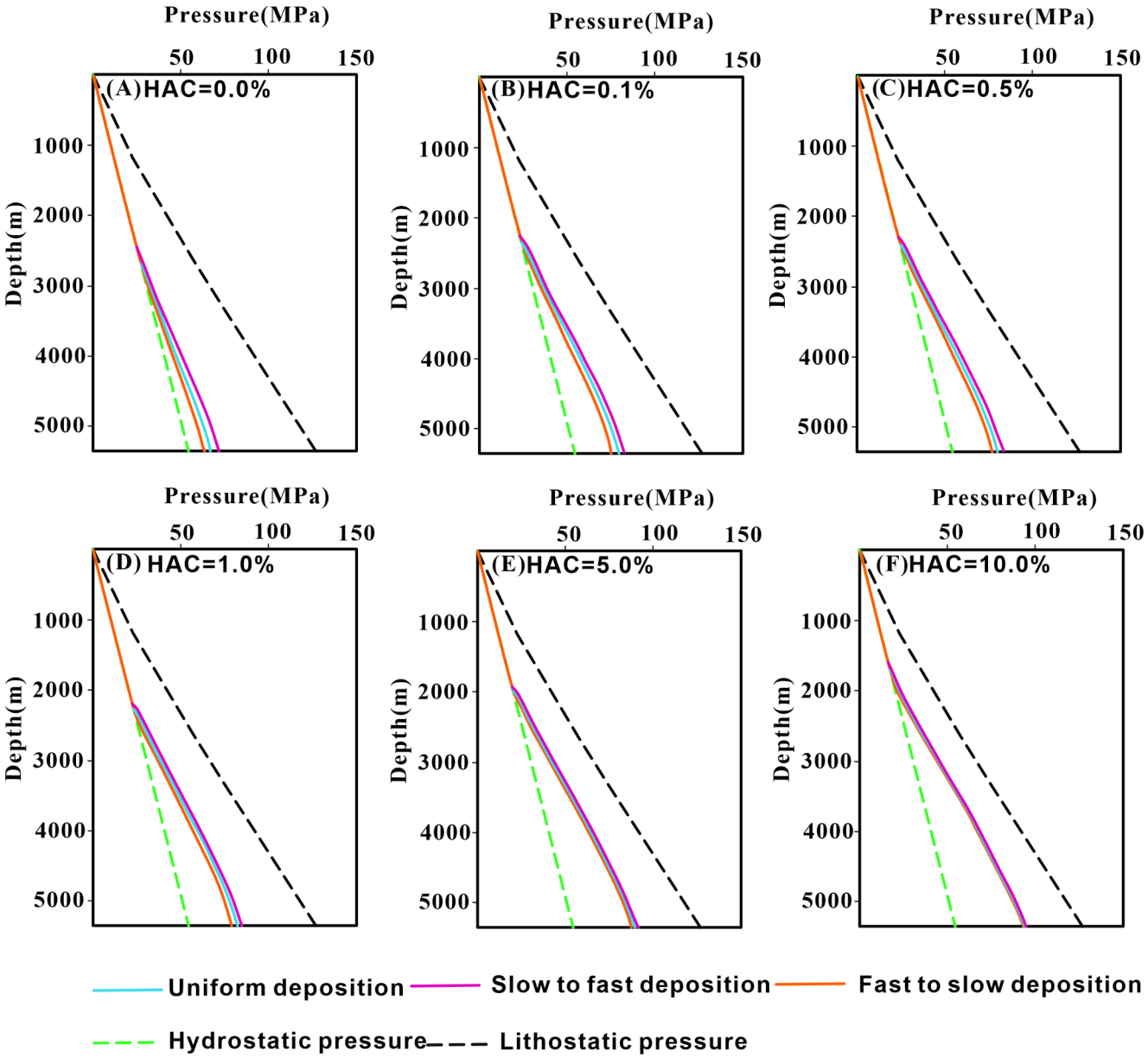

Fig. 8 Fluid pressure curve characteristics of different halite contents under different deposition mode when the SHC = 80%: (**A**) HAC = 0.0%; (**B**) HAC = 0.1%; (**C**) HAC = 0.5%; (**D**) HAC = 1.0%; (**E**) HAC = 5.0%; (**F**) HAC = 10.0%

minerals, and other minerals is derived from the average of multiple data acquired from the X-ray Diffraction (XRD) of a single well core.

Table 2 presents the mineral composition of E_3^2 in each well in this case. The content of halite developed in well Tu 2 and Chaiye 2 is 2.81% and 3.65%, respectively. However, the content of clay minerals in well Tu 2 and Chaiye 2 is 61.98% and 66.88%, respectively. The calculation results indicates that the depositional rate of both wells Tu 2 and Chaiye 2 can be divided into two stages. During 53.5 Ma~24.6 Ma, although there was a short period of rapid deposition, the formation mostly experienced slow depsition. However, from 24.6 Ma to present, the strata were rapidly deposited at a rate of more than 200 m/Ma (Fig. 10a and b). Further, the deposition mode of well Fengzhong 4 is first slow followed fast, while that of well Nan 14 is first fast followed slow (Fig. 10c and d).

According to the simulation results in the software, the intensity of formation overpressure in the wells can be as follows: Chaiye 2>Tu 2>Fengzhong 4>Nan 14. To verify these simulation results, the equilibrium depth method was used to estimate the formation pressure in the well. Firstly, a normal compaction curve was established in wells based on the characteristics of the acoustic time difference of the

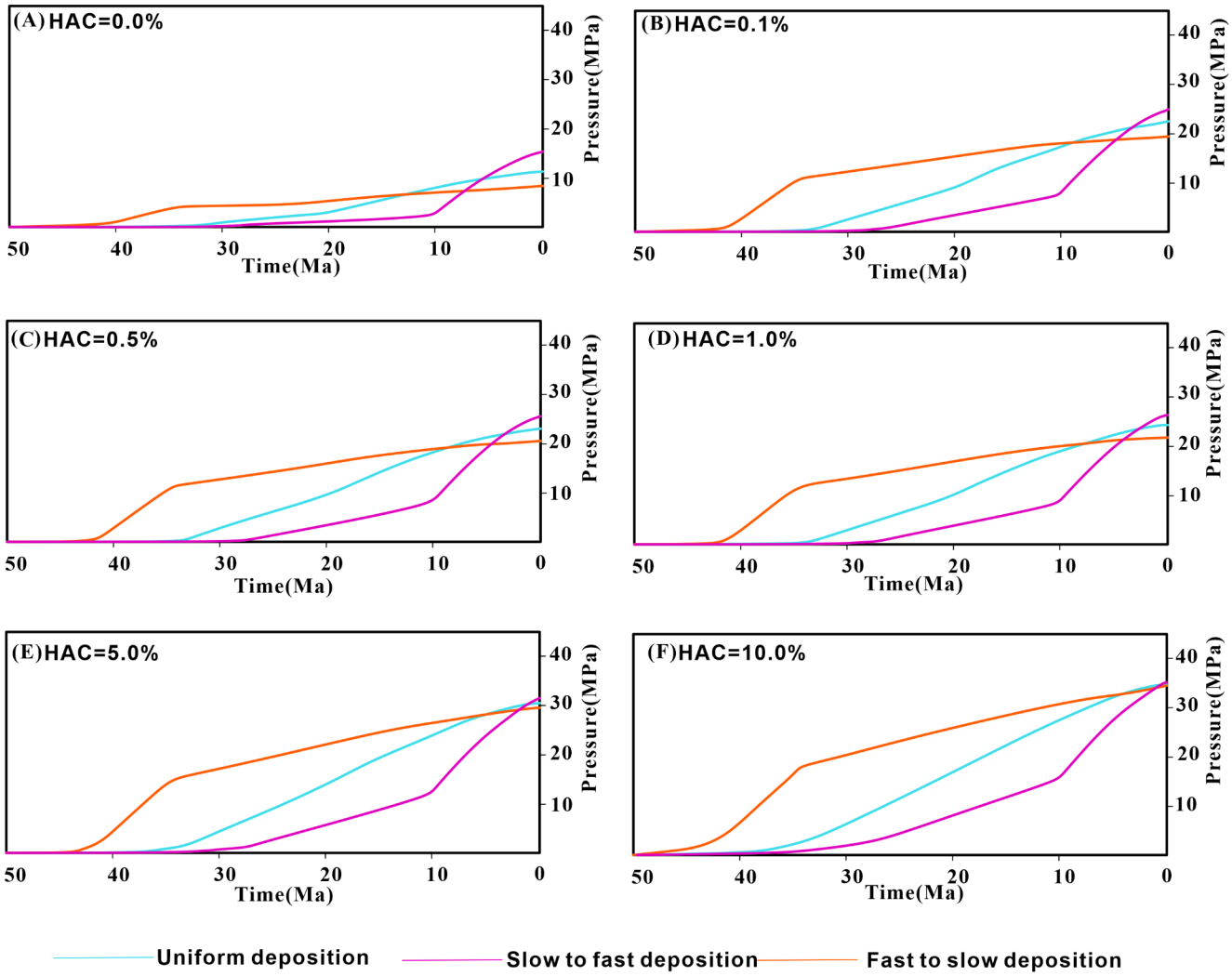

Fig. 9 Fluid pressure evolution characteristics of thin layer A under different deposition mode with different halite contents at 80% shale content: (**A**) HAC = 0.0%; (**B**) HAC = 0.1%; (**C**) HAC = 0.5%; (**D**) HAC = 1.0%; (**E**) HAC = 5.0%; (**F**) HAC = 10.0%

Table 2 Average values of rock mineral composition in wells Tu 2, Chaiye 2, Fengzhong 4 and Nan 14 in the Western Qaidam basin

Well	horizon	Clay minerals content/%	halite content/%	Other minerals content/%
Tu 2	E_3^2	61.98	2.81	35.21
Chaiye 2	E_3^2	66.88	3.65	29.47
Fengzhong 4	E_3^2	68.21	0%	31.79
Nan 14	E_3^2	71.67	0%	28.33

shale in the normal compaction section. Then, the effective stress of the well is calculated according to the principle of effective stress proposed by Magara, which states that if the time difference of sound waves in the same well is equal, the effective stress will also be equal. Finally, the fluid pressure is calculated from the lithostatic pressure and the effective stress. Figure 11 illustrates the fluid pressure calculations for wells Tu 2, Chaiye 2, Fengzhong 4 and Nan 14. The strength of overpressure is determined by the deviation of the fluid pressure curve from the hydrostatic pressure curve. Additionally, the greater the distance between the fluid pressure curve and the hydrostatic pressure curve indicates a greater strength of overpressure. The calculation results show that the overpressure strength of wells Tu 2 and Chaiye 2 is greater than the well Fengzhong 4 and Nan 14, indicating that high overpressure is likely to be formed when the formation contains halite. Both well Fengzhong 4 and Nan 14 contain no halite and have nearly the same mud content and average deposition rate, but produce different overpressure results. We believe that the difference in depositional mode between wells Fengzhong 4 and Nan 14 is the main contributing factor to this result. In other words, the results from the actual well align with the conclusions derived from the software simulation.

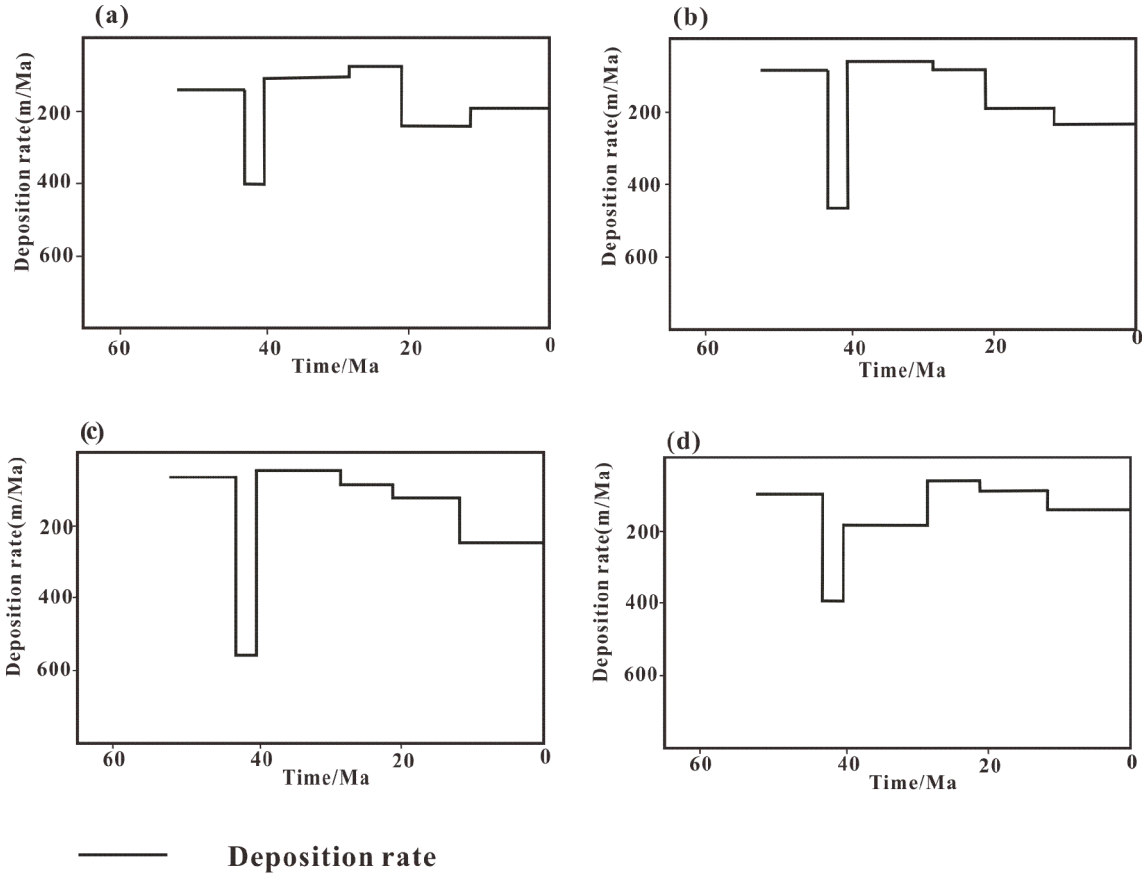

Fig. 10 Sedimentation rates of Tu 2, Chaiye 2, Fengzhong 4 and Nan 14 wells in the western Qaidam Basin

The effect of gypsum rock on overpressure

In sedimentary basins, gypsum rock is considered to be a good seal in the formation of overpressure. In the regions where large sets of thick layers of gypsum rock are extensively developed, the subsalt exhibits high strength of overpressure (Kukla et al. 2011; Li et al. 2021; Wang et al. 2022). The upper member of the lower Ganchaigou Formation in the Yingxi area of the western Qaidam Basin has a significant occurrence gypsum rock. Therefore, we have chosen well S 35 and S 23 from the Yingxi area, as it provides more measured data, and employed basin simulation software to analyze the pressure distribution characteristics. It should be noted that well S 35 is located in the depositional center of the thick gypsum rock layer, while well S 23 is located at the edge of the deposition in Yingxi area. Furthermore, the thickness and distribution of the gypsum rock in the the simulated well were derived from logging interpretation, and the measured pressure values constrained the final pressure. The measured pressure coefficient at the highest point in S35 reaches 2.08, while the minimum coefficient is 1.82. The measured pressure coefficient of the smallest measurement point S 23 can also reach 1.38.

Figure. 12 shows the distribution locations of the gypsum formations and the simulation results of the present pressure distribution characteristics in well S 35 and S 23. The results show that there are two pressure systems in well S35 and well S23, normal pressure and overpressure. The gypsum rock formation often acts as a boundary where overpressure rapid increases. In order to analyze the sealing effect on overpressure, the pressure difference between the top and the bottom interface of the gypsum rock is used to judge the sealing ability of overpressure. It is evident that the greater the pressure difference, the stronger the sealing ability of the gypsum rock. Table 3 shows the residual formation pressure difference between the top and bottom boundaries of each gypsum rock in well S 35 and S 23, along with the average depth and thickness of gypsum rock. The fitting curve between gypsum rock thickness and fluid pressure difference indicates a good positive correlation with a fitting degree above 0.9 (Fig. 13). This correlation is reasonable since thicker gypsum rock presents a longer barrier for fluid to escape, resulting in more fluid being trapped in the formation and generating stronger overpressure. In other words, the thicker the gypsum rock exhibits better sealing ability for overpressure.

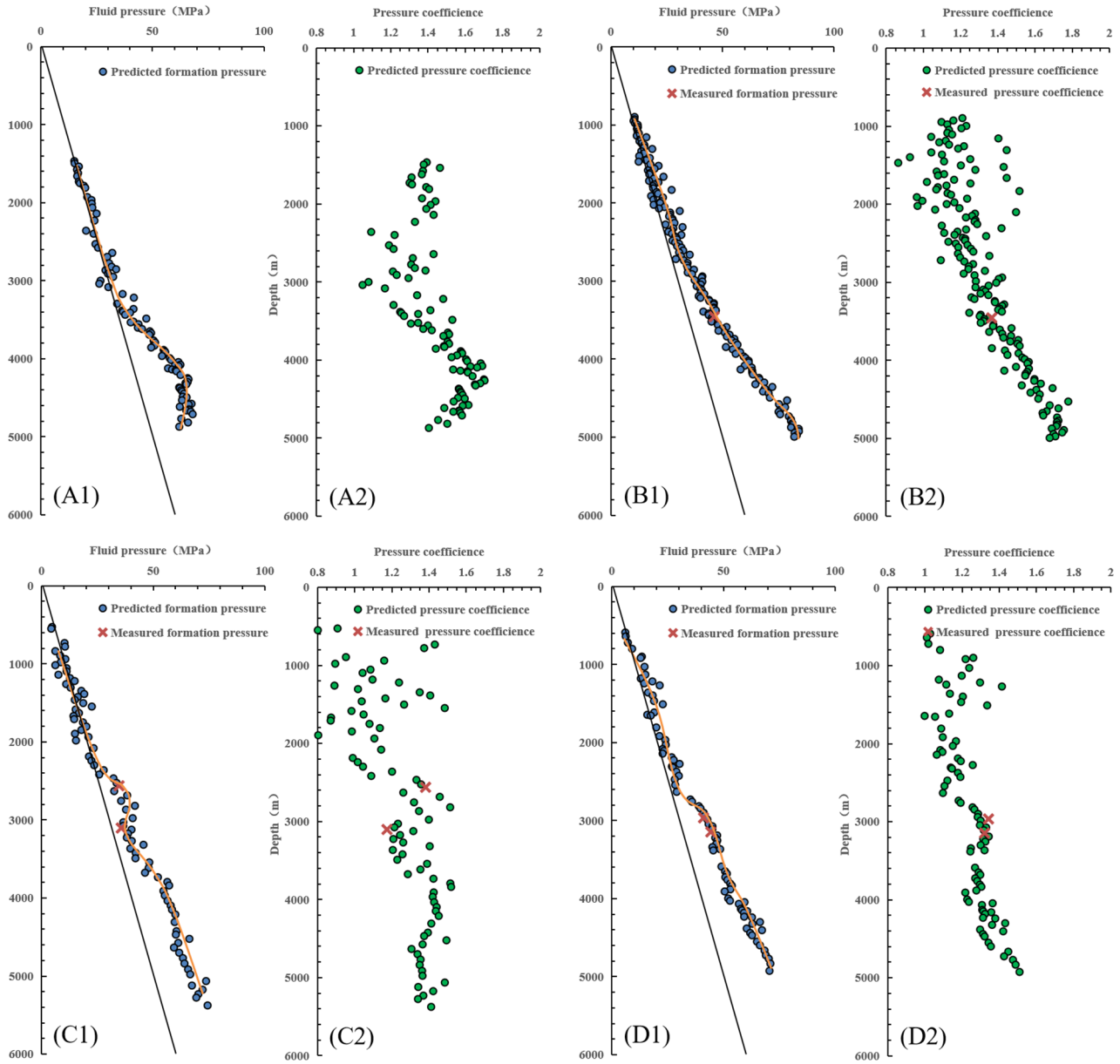

Fig. 11 Pressure Curve Characteristics of Wells Tu 2, Chaiye 2, Fengzhong 4 and Nan 14 in the Western Qaidam Basin. (A1 and A2) well Tu 2; (B1 and B2) well Chaiye 2; (C1 and C2) well Fengzhong 4; (D1 and D2) well Nan 14

Due to the limitation of the software, the change of sealing property caused by gypsum rock creep damage is not considered. However, cracks and microcracks commonly develop during the creep stage of the gypsum rock. These cracks tends to propagate along the initial microcrack tip, eventually connect and converge to form fractures (Wang et al. 2022). For example, in Campos Basin (Brazil), located the eastern margin of South America, the creep of gypsum rock leads to the generation of plastic faults, which provides a channel for the migration adjustment of oil and gas under the regional cap of the gypsum rock to the supersalt zone (Guo et al. 2019).

In summary, we propose that halite influences the development of formation overpressure by cementing and filling pores during deposition, thereby disrupting the original pore structure. This process reduces the permeability of the formation, impedes fluid expulsion, and ultimately leads to the formation of overpressure. Additionally, if the formation experiences an extreme evaporation event during deposition (e.g., the upper section of the Xiaganchaigou Formation in the Yingxi area of the western Qaidam Basin), the resulting highly compacted gypsum layer can serve as an effective pressure seal, aiding in the preservation of overpressure.

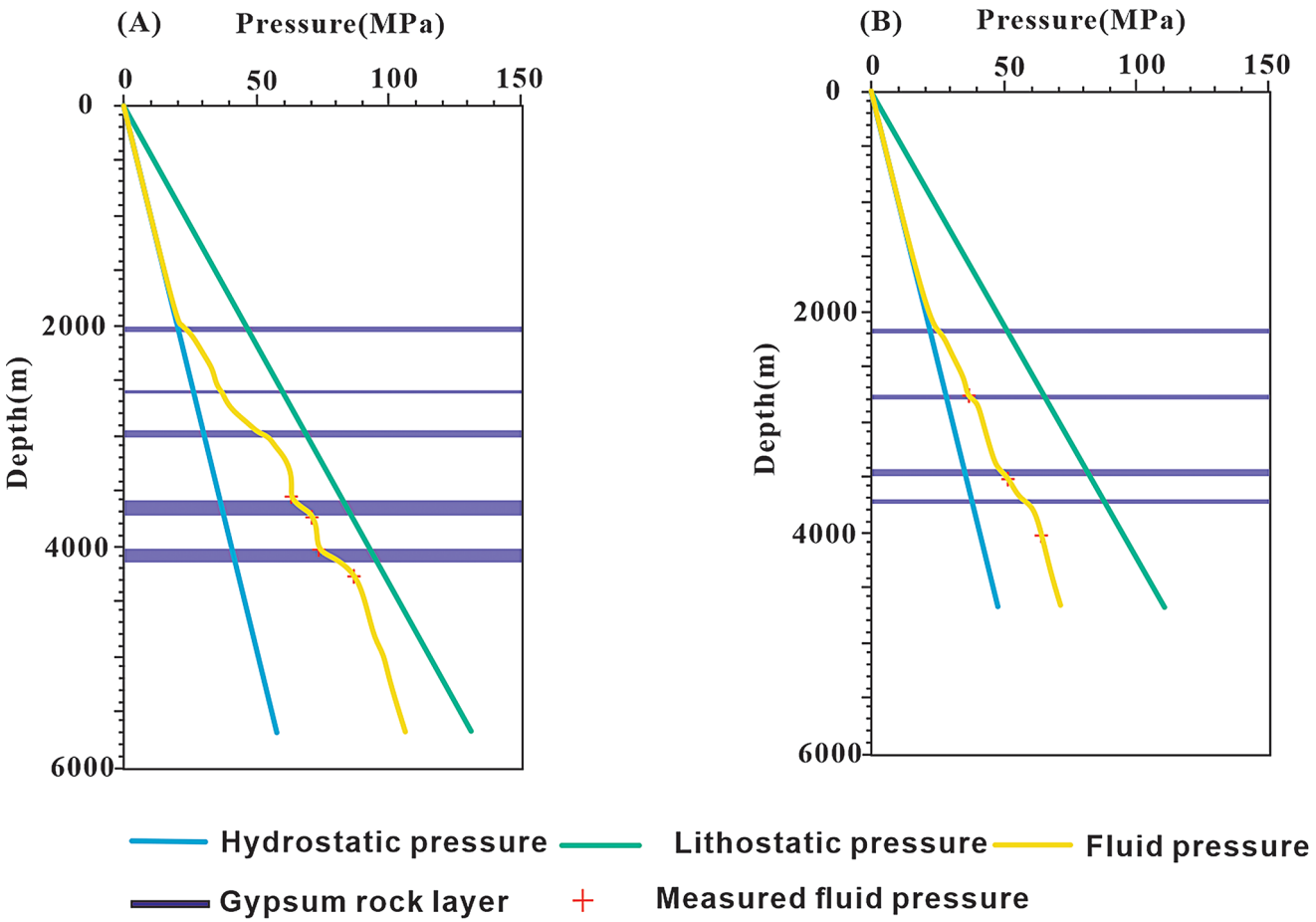

Fig. 12 Fluid pressure curve and distribution characteristics of gypsum rocks in the Yingxi area of the Qaidam Basin: (**A**) well S 23; (**B**) well S 35

Table 3 .Simulation results of gypsum layer thickness and overpressure in wells S23 and S35

Well	Depth of gypsum salt layer/m	Gypsum rock thickness/m	Cumulative gypsum salt thickness/m	Cumulative overpressure/MPa	Cumulative pressure coefficient
SHI 23	2051	42	42	4.31	1.21
SHI 23	2635	20	62	11.30	1.44
SHI 23	3010	61	123	24.74	1.84
SHI 23	3732	123	246	34.10	1.93
SHI 23	4159	126	366	40.94	2.00
SHI 35	2199	28	28	4.55	1.21
SHI 35	2896	20	48	9.92	1.35
SHI 35	3491	68	116	16.47	1.48
SHI 35	3748	24	140	22.42	1.61

Model limitations

Section 3.1 highlights the effect of rock composition on custom rock compaction curves and porosity-permeability characteristics. However, the models developed in Sect. 3.2, 3.3, and 3.4 emphasize the influencing factors of overpressure during the deposition of rock on the depositional profile. These factors include differences of rock composition, depositional rate, and the depositional mode in the simulation process. The advantage of this model is that it disregards the influence of overburden, tectonic compression, hydrocarbon generation, and pressure transfer on the fluid pressure. In other words, the overpressure studied in this model is solely attributed to disequilibrium compaction. Section 3.5 discusses the sealing effect of layered gypsum rock on fluid pressure. The gypsum layer is a kind of plastic fluid, so it is necessary to consider the plastic flow behavior of halite during geological history, and obtain the

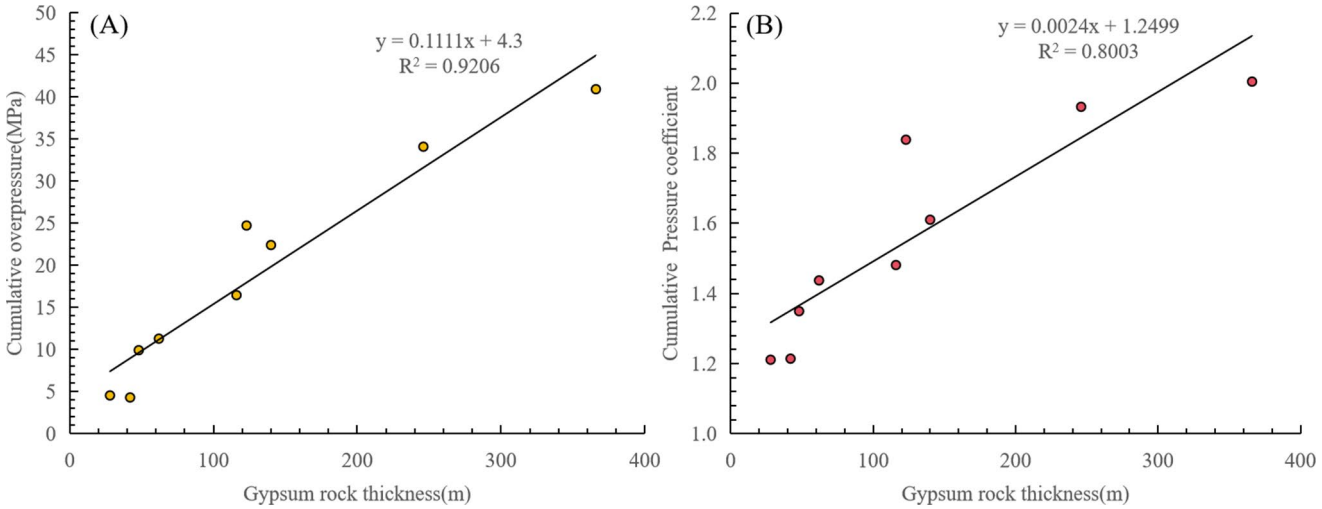

Fig. 13 Relationship between cumulative gypsum thickness and pressure.: (**A**) Cumulative gypsum thickness-Cumulative overpressure; (**B**) Cumulative gypsum thickness-Pressure coefficient

ancient geometric structure of the present gypsum layer. In addition, the viscous behavior of the gypsum rock alters the stress distribution during tectonic compression and locally redistributes the mean stress within the gypsum layer, thus affecting the pressure distribution. However, in the inversion process of this study, gypsum rocks are simplified as a regionally effective overpressure seal with very low permeability. Of course, this model is simplified because mechanical compression is one of the main causes of fluid pressure generation and permeability reduction. Other phenomena should be considered at greater depths, such as the transformation of limonite in shale, the cementation of sandstone, and any chemical transformation of sediment (Luo and Vasseur 1996, 2016).

Another complexity of fluid properties must be emphasized: fluid in pores is assumed to be pure water with low compressibility throughout the study. Therefore, in the Biot effective stress coefficient equation, the bulk elastic modulus of rocks only considers the compressibility of the sediment volume. However, in reality, when hydrocarbons are present in the pores, the compressibility of the actual fluid can be significantly higher, thereby affecting the final bulk elastic modulus of the rock. In addition, the increased fluid volume associated with oil and gas production can observe as an important mechanism for overpressure if the hydrocarbon maturation process in shale is active (Luo and Vasseur 1996; Surdam et al. 1994). In extreme cases, such as when the system is saturated with highly compressible gas, the expansion of gas may compensate for fluid losses during hiatus and even during erosion (Liu et al. 2016). The formation will also squeeze the formation fluid during the tectonic compression process, which significantly improves the compressibility of the formation fluid. In other words, since tectonic compression and hydrocarbon generation were not taken into account, the impact of halite on formation overpressure in the under-compacted field in this simulation was estimated to be too large. Modeling such complex phenomenon requires the use of basin models to explain the simultaneous evolution of various physicochemical processes.

Finally, one of our basic assumptions is that the lithology remains uniform across the sedimentary profile, considering the custom rock composed of shale, sandstone, and halite. However, if there is a significant lithology change, the fluid pressure field will be significantly different. For example, if the shale-sandstone interface gradient is severe, the true extent of the permeate may be greater than that of the reservoir (Luo and Vasseur 1992). In actual sedimentary basins, strata accumulation is rarely a simple proportional combination of shale, sandstone, and halite. Instead, it typically occurs in the form of thick layers, interlayers, thin layers, or other single-lithology deposits. Moreover, the heterogeneity of strata in real sedimentary basins is often significant. Factors such as intermittent stratigraphic deposition, changes in sedimentary facies, structural inversion of strata, diagenesis, and faults can all influence simulation outcomes. Therefore, the results of this simulation reflect a semi-quantitative general trend and should not be interpreted as precise quantitative findings. Despite its limitations, this approach provides a rapid and quantitative method that effectively captures the influence of rock composition, depositional rate, and depositional methods on overpressure.

Conclusion

This study shows that halite reduces the original porosity and permeability of shale and sandstone by blocking the pores in the formation, thus changing the compaction

process of the rock. In other words, halite changes the compaction behavior of shale-sand layers.

The M/L is one of the important factors affecting formation overpressure. For shale-sand layers, halite has a positive effect on the development of overpressure, which is mainly reflected in two aspects: (1) under the same deposition conditions, the HAC is positively correlated with the intensity of overpressure. (2) Halite reduces the threshold of deposition conditions for the formation of undercompacted overpressure.

When the DR is changed, the shale-sandstone layer shows the highest overpressure intensity when the deposition rate is the largest. when the deposition mode is changed, the deposition that is slow first and then fast shows the highest overpressure intensity. However, when the formation contains halite, the positive effects of deposition rate and deposition mode on overpressure are weakened.

The thickness of gypsum rock is positively correlated with the excess pressure difference in the gypsum layer. This is because the thicker the gypsum rock, the longer the barrier for fluids to escape, causing more fluids to be trapped in the formation, creating a stronger overpressure.

Supplementary Information The online version contains supplementary material available at https://doi.org/10.1007/s13146-025-01087-z.

Acknowledgements The author sincerely thanks the support of the National Natural Science Foundation of China (41872127) and the guidance of Professor Mei Jinshun.

Author contributions All authors discussed the results and contributed to the final manuscript.Taozheng Yang: Conceptualization, Methodology, Data curation, Formal analysis, Writing-Original Draft, Writing - Review & Editing.Chenglin Liu: Supervision, Funding acquisition, Project administration, Visualization, Writing-Review & Editing.Jixian Tian: Conceptualization, Validation, Writing-Review & Editing. Rizwan Sarwar: Writing-Review & Editing.Guoxiong Li: Data curation, Investigation. Zhengang Ding: Resources, Data curation.Hongliang Huo: Resources, Data curation.Yubo He: Investigation.Haidong Wang: Investigation.Tong Qiao: Investigation.

Data availability No datasets were generated or analysed during the current study.

Declarations

Competing interests The authors declare no competing interests.

References

Athy LF (1930) Density, porosity, and compaction of sedimentary rocks. AAPG Bull 14(1):1–24

Audet D, McConnell J (1992) Forward modelling of porosity and pore pressure evolution in sedimentary basins. Basin Res 4(2):147–162

Broichhausen H, Littke R, Hantschel T (2005) Mudstone compaction and its influence on overpressure generation, elucidated by a 3D case study in the North sea. Int J Earth Sci 94(5–6):956–978

Cao H, Gong JJ, Wang GF (2006) The cause of overpressure and its relationship with reservoir forming. Nat Gas Geoscience 24(6):1935–1945

Dickinson G (1953) Geological aspects of abnormal reservoir pressures in the Gulf Coast region of Louisiana. U S AAPG Bull 37(2):410–432

Du X, Zheng HY, Jiao XQ, China Universitys of Geosciences, Beijing (1995) Abnormal pressure and oil and gas distribution. Earth Sci Front 2(4):12

Fan C, Wang G (2021) The significance of a piecemeal geometric model of mudstone compaction: Pinghu slope, Xihu depression, Eastern China. Mar Pet Geol 131:105138

Fan CY et al (2016) Identification and calculation of transfer overpressure in the Northern Qaidam basin, Northwest China. AAPG Bull 100(1):23–39

Feng C, Cai H (2014) Seepage mechanics mechanism of undercompacted mudstone's formation. Appl Mech Mater 459:693–697

Guo P et al (2018) Palaeohydrological evolution of the late cenozoic saline lake in the Qaidam basin, NE Tibetan plateau: tectonic vs. climatic control. Global Planet Change 165:44–61

Guo P et al (2019) Geochemical behavior of rare elements in paleogene saline lake sediments of the Qaidam basin, NE Tibetan plateau. Carbonates Evaporites 34:359–372

Hantschel T, Wygrala B, Fuecker M, Neber A (2012) Modeling basin-scale geomechanics through geological time, IPTC 2012: International Petroleum Technology Conference. EAGE Publications BV, pp. cp-280-00289

Hunt JM (1990) Generation and migration of petroleum from abnormally pressured fluid compartments. AAPG Bull 74(1):1–12

Kukla PA, Reuning L, Becker S, Urai JL, Schoenherr J (2011) Distribution and mechanisms of overpressure generation and deflation in the late neoproterozoic to early cambrian South Oman salt basin. Geofluids 11(4):349–361

Li XQ, Zhao YC (2012) Overpressure genesis in the Liutun salt-lake Sag,Dongpu depression,bohai Bay basin. Oil Gas Geol 33(05):686–694 (in Chinese with English abstract)

Li J, Tang Y, Tao WU, Zhao J, Bai Y (2020) Overpressure origin and its effects on petroleum accumulation in the conglomerate oil Province in Mahu Sag, Junggar basin, NW China. Pet Explor Dev 47(4):726–739

Li P et al (2021) Characteristics and genetic mechanism of layer overpressure in saline lake basin: A case study of oligocene in Yingxi area, Qaidam basin. J China Univ Min Technol 50(01):917–929 (in Chinese with English abstract)

Liu CL et al (2016) Geochemical characteristics of the paleogene and neogene saline lacustrine source rocks in the Western Qaidam basin, Northwestern China. Energy Fuels 30(6):4537–4549

Liu H et al (2017) Overpressure characteristics and effects on hydrocarbon distribution in the Bonan Sag, Bohai Bay basin, China. J Petroleum Sci Eng 149:811–821

Liu H, Wang Y, Jiang Y, Yuan F, Guo Z (2019a) Quantification models of overpressuring in paleogene source rocks of the Raoyang depression, Bohai Bay basin, China. Mar Pet Geol 109:607–622

Liu H et al (2019b) Mechanisms for overpressure generated by the undercompaction of paleogene strata in the Baxian depression of Bohai Bay basin, China. Mar Pet Geol 99:337–346

Liu JD, Liu T, Jiang YL, Wan T, Liu RN (2019c) Distribution, origin, and evolution of overpressure in the Shahejie formation of Northern Dongpu depression, Bohai Bay basin, China. J Petroleum Sci Eng 181:106219

Liu WB et al (2020) Formation of inter-salt overpressure fractures and their significances to shale oil and gas: A case study of the third

member of paleogene Shahejie formation in Dongpu Sag, Bohai Bay basin. Pet Explor Dev 47(03):523–533
Luo X, R (2000) Application of numerical value basin modeling method in soil quality research. Pet Explor Dev 27(2):6–10
Luo XR (2004) Quantitative analysis of overpressure mechanism of tectonic stress. Geophys J 47(6):1086–1093 (in Chinese with English abstract)
Luo X, Vasseur G (1992) Contributions of compaction and aquathermal pressuring to geopressure and the influence of environmental conditions. AAPG Bull 76(10):1550–1559
Luo X, Vasseur G (1996) Geopressuring mechanism of organic matter cracking: numerical modeling. AAPG Bull 80(6):856–873
Luo X, Vasseur G (2016) Overpressure dissipation mechanisms in sedimentary sections consisting of alternating mud-sand layers. Mar Pet Geol 78:883–894
Luo X, Wang Z, Zhang L, Yang W, Liu L (2007) Overpressure generation and evolution in a compressional tectonic setting, the Southern margin of Junggar basin, Northwestern China. AAPG Bull 91(8):1123–1139
Neuzil C, Pollock D (1983) Erosional unloading and fluid pressures in hydraulically tight rocks. J Geol 91(2):179–193
Osborne MJ, Swarbrick RE (1997) Mechanisms for generating overpressure in sedimentary basins: A reevaluation: reply. AAPG Bull 90(81):1023–1041
Ramdhan AM, Goulty NR (2010) Overpressure-generating mechanisms in the Peciko field, lower Kutai basin, Indonesia. Pet Geosci 16(4):367–376
Ramdhan AM, Goulty NR (2018) Two-step wireline log analysis of overpressure in the Bekapai field, lower Kutai basin, Indonesia. Pet Geosci 24(2):208–217
Shi JN, Jiang JQ, Chen FX, Zhong GG (2015) Forming mechanism of overpressure and its significance on hydrocarbon accumulation in Damintun Sag. J Jiling University(Earth Sci Edition) 35(6):745–750 (in Chinese with English abstract)
Su A, Chen H, Ping H, Lei M, Wang C (2019) Paleo-pressure evolution and its origin in the Pinghu slope belt of the Xihu depression, East China sea basin. Mar Pet Geol 107:198–213
Surdam RC, Jiao ZS, Martinsen RS (1994) The regional pressure regime in cretaceous sandstones and shales in the powder river basin. Pet. Geol. Mem.
Tingay M et al (2013) Evidence for overpressure generation by kerogen-to-gas maturation in the Northern Malay basin. AAPG Bull 97(4):639–672
Wang Y et al (2011) Cenozoic uplift of the Tibetan plateau:evidence from tectonic-sedimentary evolution of the Western Qaidam basin. Earth Sci Front 18(3):141–150
Wang BJ et al (2012) Effective stress characteristics of different overpressured origins in Dongying depression of the Bohai Bay Basin,China. Geol Sci Technol Inform 31(2):72–79 (in Chinese with English abstract)
Wang B, Qiu N, Amberg S, Duan Y, Littke RJM (2022) Modelling of pore pressure evolution in a compressional tectonic setting: the Kuqa depression, Tarim basin, Northwestern China. Mar Pet Geol 146:105936
Yang B et al (2015) Shale compaction and overpressure distribution in Southeast slope of Dongying Sag,Bohai Bay basin. Xinjiang Petroleum Geology
Zhang J (2011) Pore pressure prediction from well logs: methods, modifications, and new approaches. Earth Sci Rev 108(1–2):50–63
Zhang JC (2013) Effective stress, porosity, velocity and abnormal pore pressure prediction accounting for compaction disequilibrium and unloading. Mar Pet Geol 45:2–11
Zhao JZ, Li J, Xu ZY (2017) Research progress of overpressure genesis in sedimentary basins. Acta Petrolei Sinica 38(09):973–998 (in Chinese with English abstract)